

## Surface and grain-boundary amorphization: Thermodynamic melting of coesite below the glass transition temperature

W. L. Gong, L. M. Wang, and R. C. Ewing

*Department of Earth and Planetary Sciences, University of New Mexico, Albuquerque, New Mexico 87131*

Y. Fei

*Geophysical Laboratory, Carnegie Institution of Washington, Washington, D.C. 10015*

(Received 14 June 1995)

Coesite, a high-pressure  $\text{SiO}_2$  polymorph, becomes amorphous during isothermal annealing below the glass transition temperature,  $T_g$ , at one-bar pressure. Transmission electron microscopy was used to examine this fusion process (vitrification) below  $T_g$ . The transformation is dominated by a heterogeneous nucleation-and-growth controlled process above the thermodynamic melting temperature,  $T_m$  (875 K), but below  $T_g$  (1480 K). Amorphous domains nucleate at free surfaces and grain boundaries, and the amorphous-crystalline interface propagates into the interior of the crystal. This "interface-mediated" amorphization (vitrification) is the same as "interface-mediated" melting, based on the thermodynamic, microstructural, and mechanistic aspects of the transformation. This amorphization process parallels electron-irradiation and pressure-induced amorphization in coesite.

There are numerous examples of crystalline-to-amorphous phase transformations in the solid state. Solid-state amorphization currently receives much attention, both experimentally and theoretically, due to the recent discovery that amorphous alloys can be produced by a variety of processes, such as by interdiffusion reactions, mechanical alloying, hydrogenation, particle irradiation, annealing of metastable phases and the application of pressure.<sup>1</sup> Two questions arise: (i) What are the common features of all these processes? (ii) What is the relationship between melting and solid-state amorphization, as both phenomena represent a periodic-to-aperiodic phase transformation.

In the case of thermodynamic melting, the phase transition involves the heterogeneous nucleation of the liquid at extended defects, such as grain boundaries, free surfaces, voids or dislocations, and a subsequent thermally activated propagation of solid/liquid interfaces through the crystal, as recently demonstrated by molecular-dynamics simulations.<sup>2-6</sup> However, mechanical melting is predicted to be homogeneous and does not require thermally activated atom mobility, as it arises from a mechanical instability limit described by the Born criterion.<sup>7</sup> Because the direct experimental evidence in support of each of these models is limited and not definitive, the question of the predominant initial mechanism for melting remains. In the case of solid-state amorphization, there is preliminary evidence in support of two types of solid-state amorphization analogous to the two types of melting. The parallels between melting and solid-state amorphization have been recently described and discussed by a number of authors.<sup>8-15</sup> For example, solid-state amorphization may proceed by a nucleation-and-growth process in electron- and ion-beam-irradiation experiments,<sup>16-18</sup> and this strongly resembles thermodynamic melting. On the other hand, there is evidence from electron irradiations at very low temperature,<sup>19</sup> hydrogenation,<sup>20</sup> and compression-induced amorphization<sup>21</sup> that solid-state amorphization occurs homogeneously. The softening of shear elastic constants before the onset of amorphization supports this view of amorphization being analogous to mechanical melting.<sup>22</sup>

To avoid ambiguity, the terms vitrification and melting are used here for the experimentally observed fusion below and above the glass transition temperature  $T_g$ , respectively.<sup>12</sup> Hence, vitrification may be useful for elucidating the parallels between amorphization and melting, from a thermodynamic and microstructural point of view. From a thermodynamic standpoint, glass formation below the glass transition temperature raises some questions, for example, whether the structure and thermodynamic properties of the amorphous phase is the same as that of an equilibrium undercooled liquid at its low formation temperature (which cannot be obtained by cooling a liquid because of the slow kinetics). Kauzmann has argued that an undercooled liquid whose entropy falls below that of the corresponding crystalline phase must undergo massive "freezing" into a glass.<sup>23,24</sup> Vitrification presents an excellent opportunity to reexamine this long-standing problem. In addition, the so called "inverse melting" or "spontaneous vitrification" are frequently used to describe the vitrification processes in intermetallic materials, such as Ti-based<sup>25-27</sup> and Nb-based<sup>28</sup> bcc alloys. Inverse melting is a polymorphous transformation of a single, homogeneous metastable crystalline phase into an amorphous phase of the same composition upon low-temperature annealing, in which the glass transition temperature  $T_g$  exceeds the melting temperature  $T_m$ .<sup>27,29-31</sup> Basically, "vitrification" and "inverse melting" describe the same phenomena. To date, there have been a number of experimental observations of vitrification or inverse melting in Ti-based and Nb-based bcc alloys,<sup>25-31</sup> and coesite and stishovite.<sup>32-35</sup> The latter two are high-pressure polymorphs of silica. However, there are experimental observations for which vitrification is not always observed (e.g., in Ti-Cr alloys).<sup>36</sup> A detailed microstructural characterization of vitrification is important to understanding microscopic mechanisms and the basic conditions which are necessary to observe the transformation. The microstructural study of vitrification not only sheds light on the mechanistic aspects of solid-state amorphization, but also provides parallel insights into the mechanisms of normal melting.

In this study, we have used transmission electron microscopy (TEM) to examine the microstructural evolution of the vitrification of coesite, a high-pressure polymorph of  $\text{SiO}_2$ , upon annealing below the glass transition temperature,  $T_g$  (1480 K), at ambient pressure. Coesite transforms into an amorphous phase under moderate heating below 1270 K.<sup>32</sup> The  $P$ - $T$  stability field of coesite is between 3.0–9.5 GPa at 1200 K. At higher pressure, coesite transforms to stishovite with six-coordinated Si, which is isostructural with rutile ( $\text{TiO}_2$ ). Coesite consists of a tetragonal framework of four-membered rings of  $\text{SiO}_4$  tetrahedra joined to form chains parallel to  $[001]$  and  $[110]$ . The large density difference between coesite ( $3.01 \text{ g/cm}^3$ ) and silica glasses ( $2.20 \text{ g/cm}^3$ ) quenched at one bar provides a good opportunity for observing the structural relationship between the amorphous phase and the initially crystalline predecessors. Skinner and Fahey,<sup>33</sup> Brazhikin *et al.*,<sup>34</sup> Grimsditch *et al.*,<sup>35</sup> and Xue *et al.*<sup>37</sup> have hypothesized that the vitrification of coesite and stishovite, is dominantly a heterogeneous nucleation-and-growth controlled process. TEM studies are required to test this hypothesis.

The coesite samples were synthesized using a piston-cylinder apparatus at 3.5 GPa and 1173 K for 48 h. The crystals are on the order of 5–10  $\mu\text{m}$  in diameter. The recovered samples from high pressure were identified by Raman spectra obtained from a micro-optical spectrometer. The bulk samples were crushed into small pieces before the annealing treatment in order to assure free surfaces on the coesite grains. The edges of the crushed pieces are transparent to 200 keV electrons, and no amorphous rim was observed before annealing. Annealing treatments of coesite were performed at 1200 K for 1, 1.5, 2.5, 3.5 h, respectively, in order to study the isothermal growth of the amorphous phase. All the specimens were observed after heat treatment under an optical microscope and then dispersed with acetone onto holey-carbon Cu grids for TEM examination. The observations were made at 200 keV using a JEOL-2000 FX analytical transmission electron microscope. Selected area and microbeam electron diffraction, as well as bright-field imaging, were employed to characterize the microstructural evolution of the vitrification process.

In the samples annealed at 1200 K for 1.5 h, amorphization (vitrification) was observed to begin at the margins of the coesite grains, as indicated by the diffuse halo diffraction pattern in Fig. 1. The amorphous/crystalline interface was sharp as revealed by conventional bright-field imaging. The amorphous layer was estimated to be 25 nm thick. The amorphous layer surrounding the coesite grains was constant in thickness. The uniform thickness of the amorphous layer suggests that amorphization occurs at a constant rate after nucleation. In addition, amorphous lamellae were also present (Fig. 2). The crystalline regions were easily recognized by the presence of bend contours, while the amorphous phase was usually featureless. Amorphous lamellae interrupt the bend contours of the crystalline regions and appear to have nucleated on the grain boundaries. Amorphized domains which nucleated on internal dislocations were not observed, nor was there evidence of homogeneous bulk amorphization. In the samples annealed at 1200 K for 3.5 h, the same features were seen, but the amorphous layer was estimated to be 60 nm in thickness. Complete amorphization of



FIG. 1. TEM bright-field image and electron-diffraction patterns from crushed coesite grains after annealing at 1200 K for 1.5 h showing amorphous layer formation at the surface. Diffraction patterns C and D were taken from the areas marked A and B in the bright-field image, respectively.

coesite at 1200 K was not observed. Only 81 vol. % of stishovite was inverted to the amorphous state after heating 3 days.<sup>37</sup>

The mechanistic aspects of amorphization (vitrification) in coesite can be summarized as (1) heterogeneous nucleation of amorphous  $\text{SiO}_2$  at surfaces and grain boundaries; (2) layer-by-layer inward growth of the amorphous region at the sharp amorphous/crystalline interface.

TEM results show that amorphization (vitrification) is definitely a heterogeneous nucleation-and-growth controlled process below the glass transition temperature ( $\sim 1480 \text{ K}$ ). In the case of crushed-grain samples, the amorphous phase nucleated at the surfaces of coesite grains. The amorphous/crystalline interface grew into the grain at a constant rate. The thickness of amorphous layer is possibly temperature dependent. These observations are consistent with those of ion-irradiation induced amorphization in silicon.<sup>18</sup> Apart from surface amorphization, the amorphous domains may have nucleated at internal boundaries, such as microtwin and subgrain boundaries. Previous authors have reported that synthetic crystals of coesite frequently contain lamellar microtwins with a twin habit plane of (010).<sup>38,39</sup> In contrast, metastable bcc Cr-Ti alloys ( $\beta\text{-Ti}_{60}\text{Cr}_{40}$ ) were found to transform during a heat treatment to a nanostructured crystalline state.<sup>36</sup>

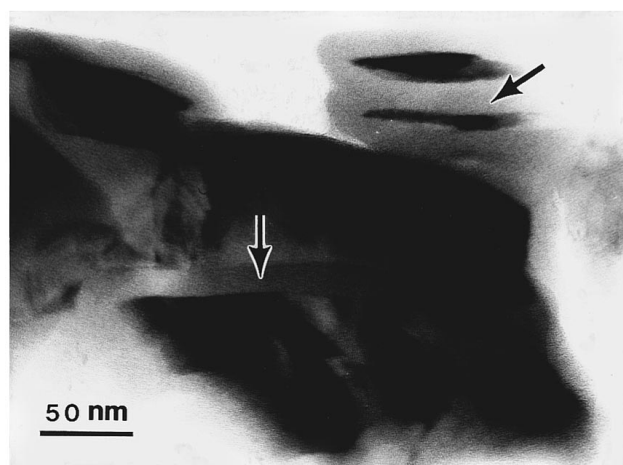


FIG. 2. TEM bright-field image of coesite after annealing at 1200 K for 1.5 h showing the amorphous lamellae at grain boundaries (arrows).

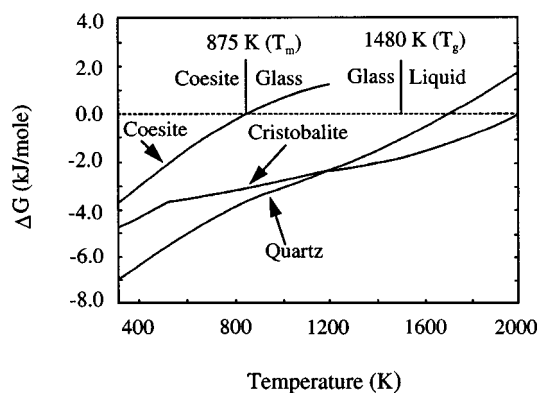


FIG. 3. The temperature dependence of free-energy differences between crystalline solids and liquids (above  $T_g$ ) or amorphous phase (below  $T_g$ ) for the  $\text{SiO}_2$  system [after Richet (Ref. 12)].

The fundamental issue in solid-state amorphization is the identification of the driving force.<sup>9,10,14</sup> When the Gibbs free energy of a crystalline phase is equal to or greater than that of the glass of the same composition at a given temperature below the glass transition temperature ( $T_g$ ), the crystalline phase becomes unstable with respect to the glass. Vitrification may occur upon annealing if the nucleation and growth of the equilibrium crystalline phase is kinetically hindered. For the  $\text{SiO}_2$  polymorphs, Gibbs free energy differences ( $\Delta G$ ) between coesite and the corresponding liquid (above  $T_g$ ) or undercooled liquid (glass, below  $T_g$ ) have been calculated based on available thermodynamic data by Richet<sup>12</sup> as shown in Fig. 3. The calculated thermodynamic melting temperature for coesite,  $\Delta G=0$  ( $T_m$ ), is estimated to be 875 K, definitely far below  $T_g$  (1480 K). If there were no kinetic limitation, at one bar coesite could thus bypass the liquid state on heating and transform directly into a glass at temperatures between 875 K and  $T_g$  (1480 K). For stishovite this must occur because stishovite is unstable with respect to  $\text{SiO}_2$  glass at all temperatures.<sup>12,34,37</sup> Apparently, the thermodynamic prediction of solid-state amorphization of coesite is consistent with our experimental observations. In the Ti-Cr system, certain temperature intervals at which  $\Delta G_{\text{cryst-glass}} \geq 0$  below their normal melting points have been suggested.<sup>13,25,29</sup> Bormann has demonstrated that a thermodynamic driving force exists for the nucleation of the amorphous phase from supersaturated Nb- and Ti-based solid solutions.<sup>31</sup> Evidently, vitrification is driven by the intrinsic thermodynamic properties of the metastable phases when they are far beyond their  $P$ - $T$  stability fields, but below  $T_g$ . The competition between nucleation and growth of equilibrium crystals and amorphous phases should determine vitrification kinetics. Theoretically above  $T_g$ , an amorphous phase is unstable as compared with a liquid. However, the kinetics of the nucleation and growth of cristobalite or tridymite are greatly favored above  $T_g$ , as reported by Dachille *et al.*<sup>32</sup>

The fundamental idea of melting is the coexistence of a solid with a liquid when the free energies of the two phases are equal. From this thermodynamic definition, vitrification and melting are the same. Amorphization occurs below  $T_g$  when the free energies of the crystal and the glass are equal, when we consider the glass as an undercooled liquid below  $T_g$ . However, the mechanistic and kinetic aspects of this

transition for vitrification, and even for melting, are still not completely understood. The original concept of surface-initiated crystal melting is very old,<sup>40</sup> but direct measurements on clean single-crystal surfaces have been possible only during the past decade.<sup>41</sup> Surface melting has been observed on an atomically clean Pb(110) surface<sup>42</sup> and Al surfaces.<sup>43</sup> The transition begins with partial disordering of the surface region (quasi-liquid layers) and progresses to a completely disordered film whose thickness increases rapidly as the temperature approaches  $T_m$ . The problem of melting at a grain boundary (GB) has long been of interest in the metallurgy. Molecular-dynamic studies show that a GB can nucleate the liquid, which then propagates through the crystal at or above  $T_m$ .<sup>3,4,9</sup> Grain-boundary melting was also directly observed in Al using a hot stage TEM.<sup>44</sup> In this study, surface and grain-boundary amorphization (correspondingly surface and grain-boundary vitrification) have been successfully observed in annealed coesite samples by TEM (Figs. 1 and 2). Thus, surface and grain-boundary amorphization (vitrification) have strong similarities to surface and grain-boundary melting. In both, the disordered or aperiodic domains nucleate at surfaces and grain boundaries and propagate through the crystal layer by layer. It has been suggested that, in the absence of nucleation centers (free surfaces or grain boundaries), a crystal can be superheated at atmospheric pressure.<sup>3,4,9</sup> Surface and grain-boundary amorphization (vitrification) of coesite occur far above  $T_m$ . Homogeneous mechanical melting (but below  $T_g$ ) is apparently suppressed and was not observed, due to the existence of free surfaces and grain boundaries. In this study, we present the direct observation of surface and grain-boundary melting far above its thermodynamic melting point (but below  $T_g$ ) and confirm the theoretically predicted results of previous studies.<sup>3,4,9</sup> Free surfaces, the simplest of all planar defects, involve excess energies. For coesite, it is expected that the first few interlayer distances are relaxed in a damped oscillatory manner and strong surface anharmonicity at the surfaces occurs with increasing temperature, as coesite is thermodynamically unstable at one bar, and there is a large volume difference between the crystal and glass. The anharmonicity manifests itself as a larger thermal-expansion coefficient in the surface region and also as an anomalous increase in the vibrational amplitudes of the surface atoms as compared to the bulk.

Coesite, as well as other tetrahedrally based polymorphs of  $\text{SiO}_2$ , including quartz, cristobalite and tridymite, can be amorphized at high pressures at room temperature. Coesite amorphizes at 30–35 GPa at 300 K.<sup>45</sup> The critical pressure at which the free energy between coesite and glass are equal was estimated to be 30–45 GPa at 300 K, in good agreement with experimental values. A molecular-dynamics study of compression-induced amorphization of  $\alpha$ -quartz suggests that the transformation is caused by the homogeneous collapse of the lattice driven by a mechanical or shear instability.<sup>46</sup> The theoretical simulations of the tetrahedrally based  $\text{SiO}_2$  polymorphs support the shear instability model for compression-induced amorphization.<sup>47–51</sup> Preliminary high-resolution transmission electron microscopy observations also favor a homogeneous mechanism.<sup>21,52</sup> Apparently, compression-induced amorphization of coesite resembles

mechanical melting. Thus coesite transforms into the amorphous state through both heterogeneous and homogeneous mechanisms, corresponding to thermodynamic and mechanical melting, respectively. In the case of vitrification, thermally activated self-diffusion plays a key role. The amorphous phase nucleates at external surfaces; this leads to surface amorphization. The propagation of the amorphous-crystalline interface requires thermally activated diffusion. In contrast, mechanical melting is difficult to observe in the laboratory without eliminating the nucleation centers. Thermodynamic melting may be hindered by either eliminating the nucleation centers or lowering the atomic mobility (for example, through compression or irradiation of the crystal at lower temperatures).<sup>9</sup> In the case of electron irradiation (200 keV and 1 MeV) of coesite at 300 K, amorphous domains nucleate heterogeneously, and amorphization is preferably initiated at interfaces, such as surfaces, the crystal-glass interface, and grain boundaries.<sup>53</sup> In the case of ion-beam irradiation (1.5 MeV Kr<sup>+</sup>), crystal-glass interfaces may be directly produced through displacement cascades in complex ceramics.<sup>54</sup>

In summary, coesite, a high-pressure SiO<sub>2</sub> polymorph, becomes amorphous during isothermal annealing at one-bar pressure. The transformation is dominated by a heteroge-

neous nucleation-and-growth controlled process above the thermodynamic melting temperature,  $T_m$  (875 K), but below the glass transition temperature,  $T_g$  (1480 K). Amorphous domains nucleate at various interfaces, e.g., free surfaces and grain boundaries. The amorphous-crystalline interfaces propagate into the crystals. This "interface-mediated" amorphization (vitrification) is the same as "interface-mediated" melting, based on the thermodynamic, microstructural, and mechanistic aspects of the transformation. Solid-state amorphization bears a strong resemblance to melting, and melting mechanisms are apparently governed by the degree of atomic mobility at the temperature at which the free energies of the crystalline and amorphous phases are equal.

The electron microscopy was completed in the Electron Microbeam Analysis Facility of the Department of Earth and Planetary Sciences at the University of New Mexico supported by NSF, NASA, DOE-BES, and the State of New Mexico. The high-pressure synthesis of coesite was completed at the Geophysical Laboratory, Carnegie Institution of Washington. This work is supported by BES/DOE Grant No. DE-FG03-93ER45498 (R.C.E.). W.L.G. particularly thanks the National Natural Science Foundation of China for support of his trip to the United States.

- <sup>1</sup>W. L. Johnson, *Prog. Mater. Sci.* **30**, 81 (1986).
- <sup>2</sup>D. Wolf, *Surf. Sci.* **226**, 389 (1990).
- <sup>3</sup>J. F. Lutsko *et al.*, *Phys. Rev. B* **40**, 2841 (1989).
- <sup>4</sup>S. R. Phillpot *et al.*, *Phys. Rev. B* **40**, 2831 (1989).
- <sup>5</sup>Y. Teraoka, *Surf. Sci.* **281**, 317 (1993).
- <sup>6</sup>P. Stoltze and J. K. Nørskov, *Surf. Sci.* **220**, L693 (1989).
- <sup>7</sup>A. R. Ubbelohde, *The Molten State of Matter: Melting and Crystalline Structure* (Wiley, Chichester, 1978).
- <sup>8</sup>W. L. Johnson *et al.*, *J. Non-Cryst. Solid* **156/158**, 481 (1993).
- <sup>9</sup>D. Wolf *et al.*, *J. Mater. Res.* **5**, 286 (1990).
- <sup>10</sup>P. R. Okamoto and M. Meshii, in *Science of Advanced Materials*, edited by H. Wiedersich and M. Meshii (Am. Soc. Met., Metals Park, OH, 1988), p. 33.
- <sup>11</sup>R. W. Cahn and W. L. Johnson, *J. Mater. Res.* **1**, 724 (1986).
- <sup>12</sup>P. Richet, *Nature (London)* **331**, 56 (1988).
- <sup>13</sup>H. J. Fecht and W. L. Johnson, *Mater. Sci. Eng. A* **133**, 427 (1991).
- <sup>14</sup>N. Q. Lam and P. R. Okamoto, *Mater. Res. Bull.* **19**, 41 (1994).
- <sup>15</sup>R. Devanathan *et al.*, *J. Alloys Compounds* **194**, 447 (1993).
- <sup>16</sup>D. E. Luzzi and M. Meshii, *Res. Mechanica* **21**, 207 (1987).
- <sup>17</sup>H. A. Atwater and W. L. Brown, *Appl. Phys. Lett.* **56**, 30 (1990).
- <sup>18</sup>H. A. Atwater *et al.*, *Nucl. Instrum. Methods Phys. Res. Sect. B* **59/60**, 386 (1991).
- <sup>19</sup>H. Mori *et al.*, *Scr. Metall.* **18**, 783 (1984).
- <sup>20</sup>W. J. Meng *et al.*, *Appl. Phys. Lett.* **53**, 1820 (1988).
- <sup>21</sup>G. H. Wolf *et al.*, in *High-Pressure Research: Application to Earth and Planetary Sciences*, edited by Y. Syono and M. H. Manghani (TERRAPUB, Tokyo/AGU, 1992), p. 503.
- <sup>22</sup>P. R. Okamoto *et al.*, *J. Less-Common Met.* **140**, 231 (1988).
- <sup>23</sup>W. Kauzmann, *Chem. Rev.* **43**, 219 (1948).
- <sup>24</sup>H. J. Fecht and W. L. Johnson, *Nature (London)* **334**, 50 (1988).
- <sup>25</sup>A. Blatter and M. von Allmen, *Phys. Rev. Lett.* **54**, 2103 (1985).
- <sup>26</sup>A. Blatter and M. von Allmen, *J. Appl. Phys.* **62**, 276 (1987).
- <sup>27</sup>Z. H. Yan *et al.*, *Phys. Rev. B* **47**, 8520 (1993).
- <sup>28</sup>R. Bormann and R. Busch, *J. Non-Cryst. Solids* **117/118**, 539 (1990).
- <sup>29</sup>A. L. Greer, *J. Less Common Met.* **140**, 327 (1988).
- <sup>30</sup>A. Blatter and J. Gfeller, *J. Less Common Met.* **140**, 317 (1988).
- <sup>31</sup>R. Bormann, *Mater. Sci. Eng. A* **179/180**, 31 (1994).
- <sup>32</sup>F. Dacheville *et al.*, *Science* **140**, 991 (1963).
- <sup>33</sup>B. J. Skinner and J. J. Fahey, *J. Geophys. Res.* **68**, 5595 (1963).
- <sup>34</sup>V. V. Brazhkin *et al.*, *J. Non-Cryst. Solids* **136**, 241 (1991).
- <sup>35</sup>M. Grimsditch *et al.*, *Phys. Rev.* **50**, 12 948 (1994).
- <sup>36</sup>C. Beeli *et al.*, *Mater. Sci. Eng. A* **179/180**, 316 (1994).
- <sup>37</sup>X. Y. Xue *et al.*, *Phys. Chem. Miner.* **19**, 480 (1993).
- <sup>38</sup>A. Bourret *et al.*, *Phys. Chem. Miner.* **13**, 206 (1986).
- <sup>39</sup>S. Sasaki *et al.*, *Z. Kristallogr.* **164**, 67 (1983).
- <sup>40</sup>Y. Teraoka, *Surf. Sci.* **294**, 273 (1993).
- <sup>41</sup>R. W. Cahn, *Nature (London)* **323**, 668 (1986).
- <sup>42</sup>J. W. Frenken, *J. Vac. Sci. Technol. A* **7**, 2147 (1989).
- <sup>43</sup>A. W. De. van der Gon *et al.*, *Surf. Sci.* **227**, 143 (1990).
- <sup>44</sup>T. E. Hsieh and R. W. Balluffi, *Acta Metall.* **37**, 1637 (1989).
- <sup>45</sup>R. J. Hemley *et al.*, *Nature (London)* **334**, 52 (1988).
- <sup>46</sup>J. S. Tse and D. D. Klug, *Phys. Rev. Lett.* **67**, 3559 (1991).
- <sup>47</sup>N. Binggeli and J. R. Chelikowsky, *Phys. Rev. Lett.* **69**, 2220 (1992).
- <sup>48</sup>N. Binggeli *et al.*, *Phys. Rev. B* **49**, 3075 (1994).
- <sup>49</sup>S. L. Chaplot and S. K. Sikka, *Phys. Rev. B* **47**, 5710 (1993).
- <sup>50</sup>J. R. Chelikowsky *et al.*, *Phys. Rev. Lett.* **65**, 3309 (1990).
- <sup>51</sup>X. Zhang and C. K. Ong, *Phys. Rev. Lett.* **48**, 6865 (1993).
- <sup>52</sup>R. R. Winters *et al.*, *Phys. Rev. Lett.* **69**, 3751 (1992).
- <sup>53</sup>W. L. Gong, L. M. Wang, R. C. Ewing, and J. Zhang (unpublished).
- <sup>54</sup>L. M. Wang and W. J. Weber, in *Microstructure of Irradiated Materials*, edited by I. M. Robertson *et al.*, MRS Symposia Proceedings No. 373 (Materials Research Society, Pittsburgh, 1995), p. 389.